

Electronic Supplementary Information

**Aggregation-Induced Phosphorescent Emission (AIPE) Behaviors in
Pt^{II}(C[^]N)(N-donor ligand)Cl-type Complexes Through Restrained *D*_{2d}
Deformation of the Coordinating Skeleton and Their Optoelectronic
Properties**

Hua Yang,^a Huiying Li,^a Ling Yue,^a Xi Chen,^a Dongdong Song,^a Xiaolong Yang,^a Yuanhui Sun,^a
Guijiang Zhou,^{a*} and Zhaoxin Wu^a

^a *School of Chemistry, MOE Key Laboratory for Nonequilibrium Synthesis and Modulation of Condensed Matter, State Key Laboratory for Mechanical Behavior of Materials, Xi'an Jiaotong University, Xi'an 710049, P. R. China.*

^b *Key Laboratory for Physical Electronics and Devices of the Ministry of Education, Faculty of Electronic and Information Engineering, Xi'an Jiaotong University, Xi'an 710049, P. R. China.*

Contents

Scheme S1	Synthetic scheme for the C [^] N-type ligands.	S4
Scheme S2	Synthetic scheme for the N-donor ligands.	S5
Fig. S1	¹ H NMR spectra for these Pt ^{II} (C [^] N)(N-donor ligand)Cl-type complexes.	S9
Fig. S2	¹³ C NMR spectra for these Pt ^{II} (C [^] N)(N-donor ligand)Cl-type complexes.	S14
Fig. S3	The TGA curves for these Pt ^{II} (C [^] N)(N-donor ligand)Cl-type complexes.	S14
Fig. S4	Photoluminescent spectra for these Pt ^{II} (C [^] N)(N-donor ligand)Cl-type complexes at 77K.	S15
Fig. S5	Particle size distribution of these Pt ^{II} (C [^] N)(N-donor ligand)Cl-type obtained from the THF : H ₂ O mixture at f_w^c .	S16
Fig. S6	CV carves for A1 , B1 , C1 , A2 , B2 , C2 , A3 , B3 and C3	S17
Fig. S7	Current density–voltage–luminance (J–V–L) relationships of the OLEDs.	S18
Fig. S8	EL efficiencies vs. luminance curves for the OLEDs.	S19

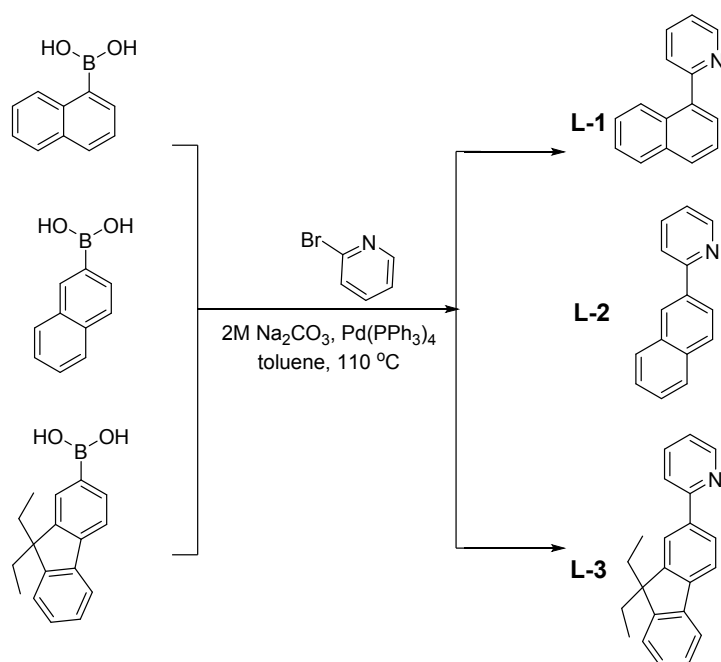
Procedures for the Synthesis of C^N-type ligands

Synthetic scheme for C^N-type ligands are shown in Scheme S1. Under the N₂ atmosphere, 1-naphthaleneboronic acid, 2-naphthaleneboronic acid or 9,9-diethyl-9H-fluorene-2-boronic acid (1.0 equiv.), 2-bromopyridine (1.2 equiv.) and Pd(PPh₃)₄ (5 mol%) were heated to 110 °C in a mixture of 5 mL of 2M K₂CO₃ and 15 mL of degassed THF for 12 h. After cooling to room temperature, the mixture was extracted with dichloromethane, the organic phase was dried with Na₂SO₄, and the solvent was removed under reduced pressure. The residue was obtained as a crude product, which was chromatographed on a silica column to produce the pure product.^{1,2}

L-1: yellowish oil; yield: 78%. ¹H NMR (300 MHz, CDCl₃, δ): 8.79 (dd, *J* = 4.8, 1.7 Hz, 1 H), 8.08 (dd, *J* = 7.1, 2.9 Hz, 1 H), 7.91 (d, *J* = 8.1, 2 H), 7.82 (dt, *J* = 7.7, 1.7 Hz, 1 H), 7.56 (m, 5H), 7.33 (ddd, *J* = 7.7, 4.8, 1.1 Hz, 1 H). ¹³C NMR (75 MHz, CDCl₃, δ): 159.5, 149.7, 138.7, 136.5, 134.2, 131.4, 129.0, 128.5, 127.6, 126.6, 126.0, 125.8, 125.4, 125.2, 122.1.

L-2: white solid; yield: 71%. ¹H NMR (300 MHz, CDCl₃, δ): 8.75 (d, *J* = 4.2 Hz, 1 H), 8.49 (s, 1H), 8.14 (dd, *J* = 8.6, 1.5 Hz, 1 H), 7.90 (m, 4H), 7.80 (td, *J* = 7.5, 1.8 Hz, 1 H), 7.50 (m, 2H), 7.26 (dd, *J* = 7.5, 4.2 Hz, 1 H). ¹³C NMR (75 MHz, CDCl₃, δ): 157.3, 149.7, 136.7, 133.5, 133.4, 128.6, 128.3, 127.6, 126.4, 126.2, 124.5, 122.1, 120.7.

L-3: white solid; yield: 77%. ¹H NMR (300 MHz, CDCl₃, δ): d 8.71 (dd, *J* = 0.8, 4.9 Hz, 1 H), 8.06 (d, *J* = 1.6 Hz, 1H), 7.59 (dd, *J* = 1.6, 7.8 Hz, 1H), 7.78–7.61 (m, 4H), 7.33–7.29 (m, 3H), 7.15–7.10 (m, 1H), 2.17–1.99 (m, 4H), 0.35 (t, *J* = 7.3 Hz, 6H). ¹³C NMR (75 MHz, CDCl₃, δ): 157.38, 150.20, 150.10, 149.30, 142.23, 140.71, 137.93, 136.36, 127.10, 126.63, 125.62, 122.66, 121.58, 121.02, 120.29, 119.71, 119.59, 56.15, 32.68, 8.55.



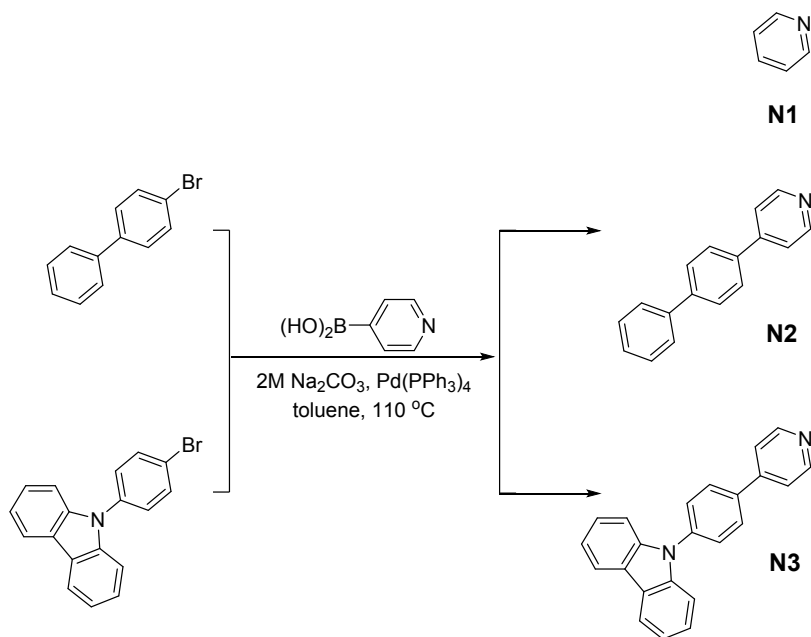
Scheme S1 Synthetic scheme for the C^N-type ligands.

Procedures for the Synthesis of N-Donor Ligands

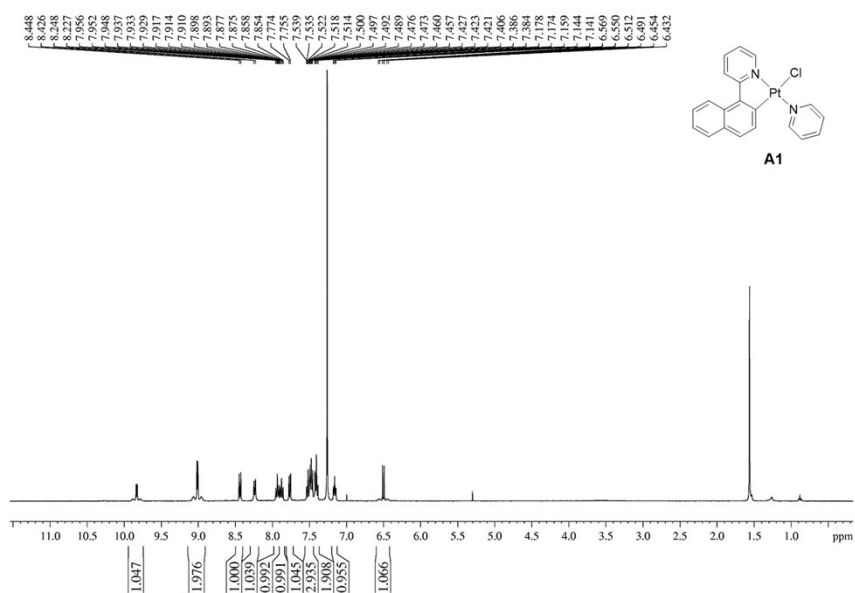
Synthetic scheme for N-donor ligands are shown in Scheme S2. Under the N₂ atmosphere, the corresponding borate compound or boronic acid (1.0 equiv.), pyridine-4-boronic acid (1.2 equiv.) and Pd(PPh₃)₄ (5 mol%) were heated to 110 °C in a mixture of 5 mL of 2M K₂CO₃ and 15 mL of degassed THF for 12 h. After cooling to room temperature, the mixture was extracted with dichloromethane, the organic phase was dried with Na₂SO₄, and the solvent was removed under reduced pressure. The residue was obtained as a crude product, which was chromatographed on a silica column to produce the pure product.^{3,4}

N2: white solid; yield: 78%. ¹H NMR (500 MHz, CDCl₃, δ): 8.68 (d, *J* = 5.5 Hz, 2H), 7.72 (s, 4H), 7.64 (d, *J* = 7.3 Hz, 2H), 7.56 (d, *J* = 6.0 Hz, 2H), 7.48 (dd, *J* = 7.6, 7.6 Hz, 2H), 7.39 (t, *J* = 7.4 Hz, 1H). ¹³C NMR (75 MHz, CDCl₃, δ): 150.2, 148.1, 142.1, 140.3, 136.9, 129.0, 127.9, 127.8, 127.5, 127.2, 121.6.

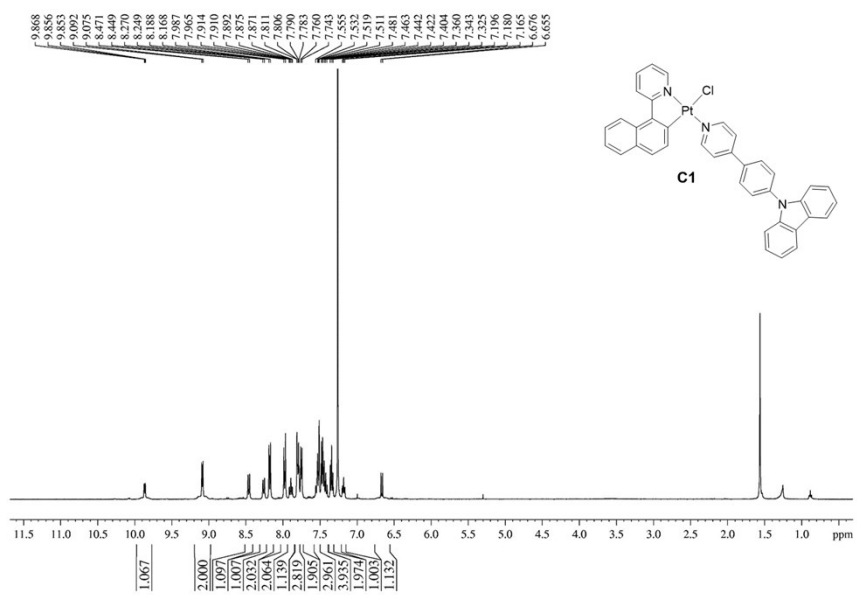
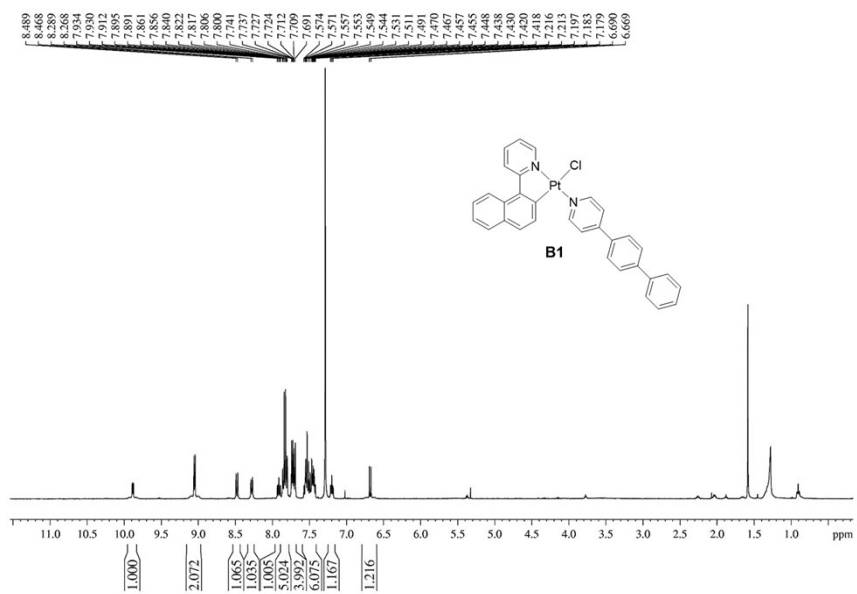
N3: white solid; yield: 68%. ¹H NMR (400 MHz, CDCl₃, δ): 8.76-8.72 (m, 2H), 8.20-8.14 (m, 2H), 7.90-7.85 (m, 2H), 7.74- 7.69 (m, 2H), 7.62-7.59 (m, 2H), 7.50-7.41 (m, 4H), 7.35-7.30 (m, 2H). ¹³C NMR (75 MHz, CDCl₃, δ): 150.6, 147.5, 140.8, 138.8, 137.2, 128.6, 127.7, 126.2, 123.7, 121.7, 120.6, 120.4, 109.9.



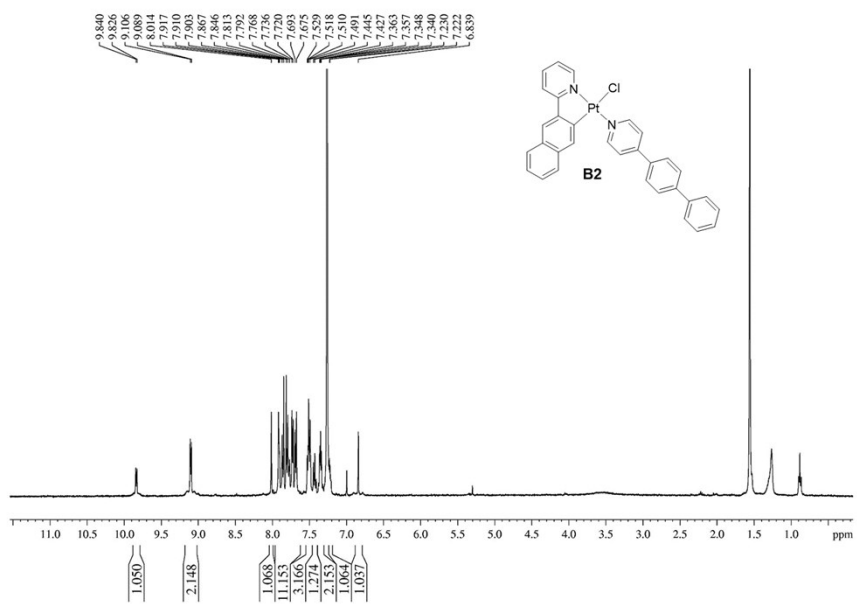
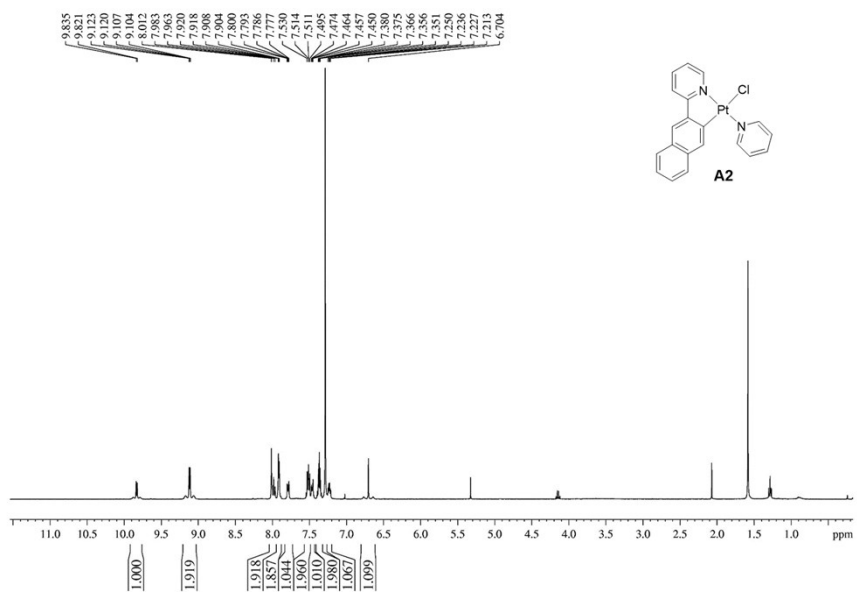
Scheme S2 Synthetic scheme for the N-donor ligands.



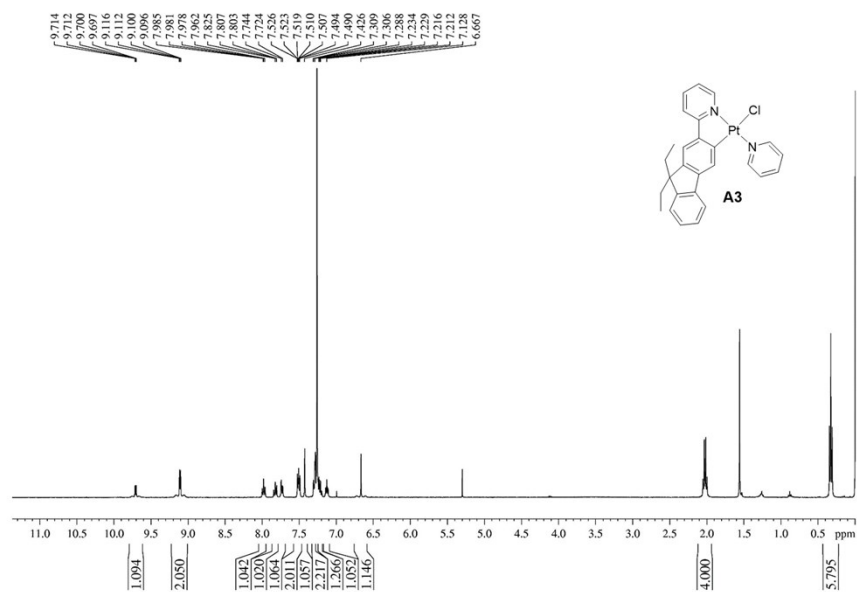
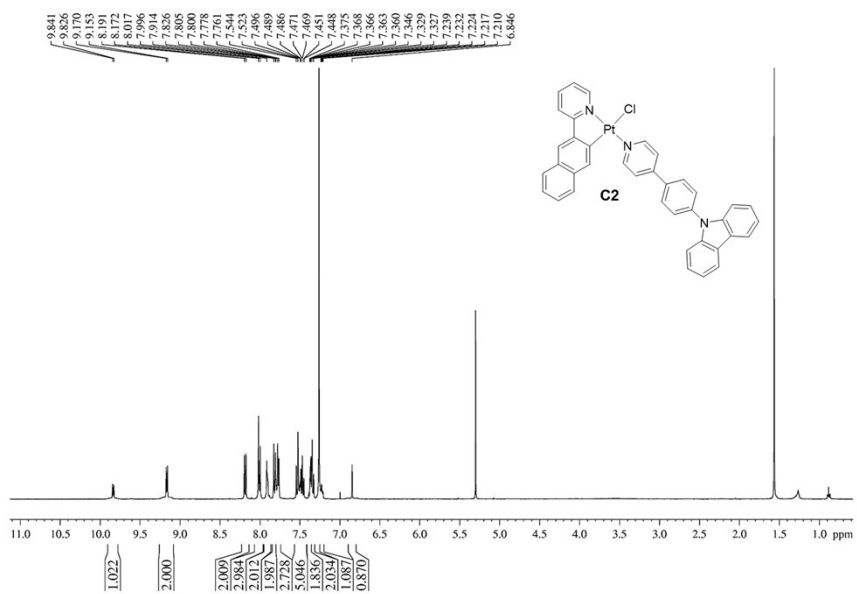
Electronic Supplementary Information



Electronic Supplementary Information



Electronic Supplementary Information



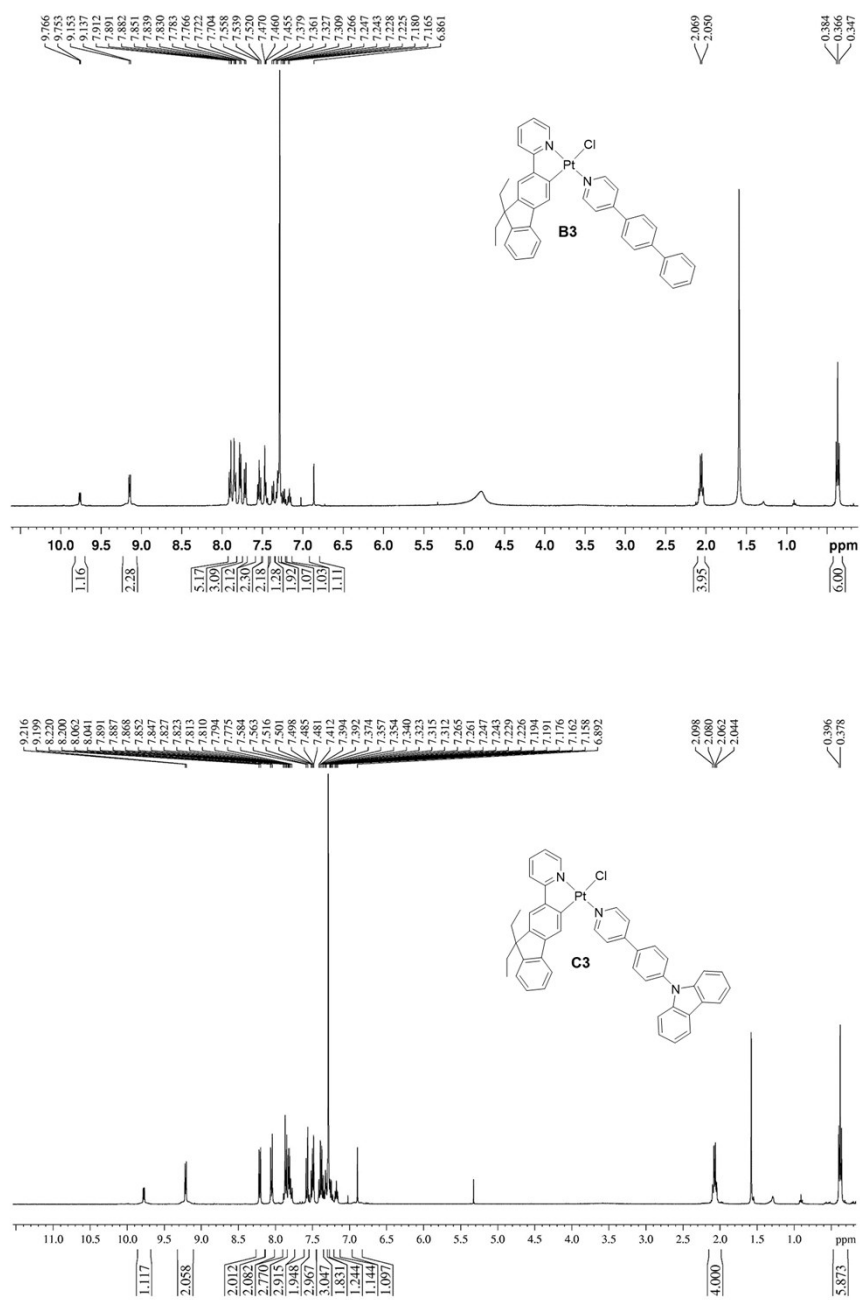
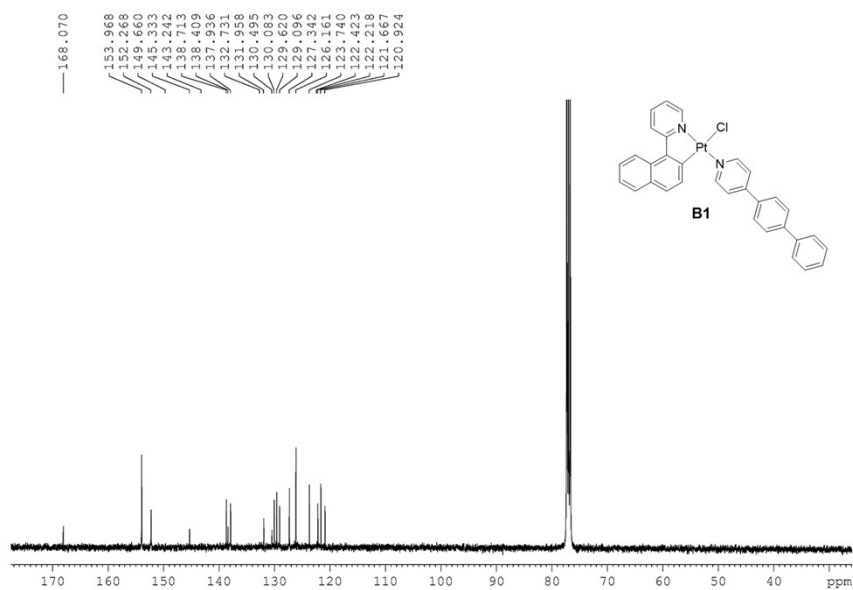
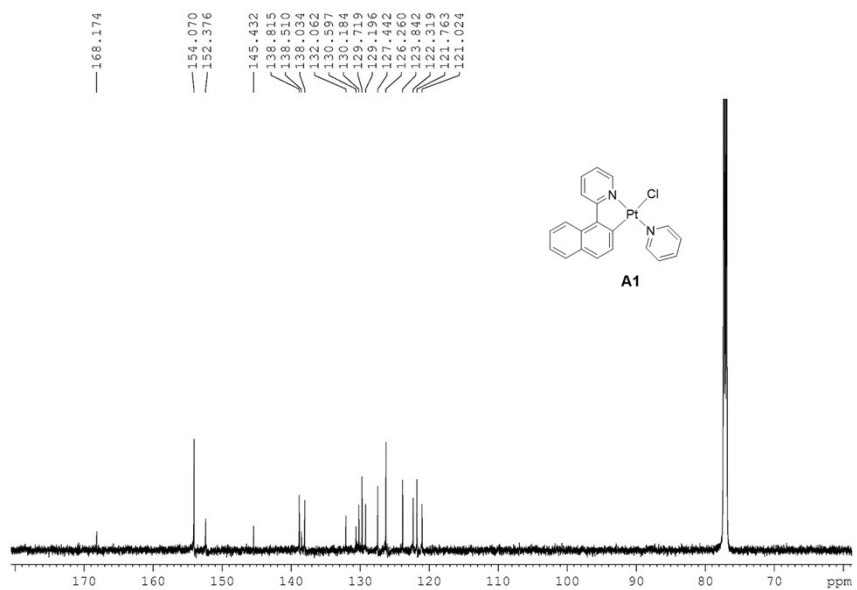
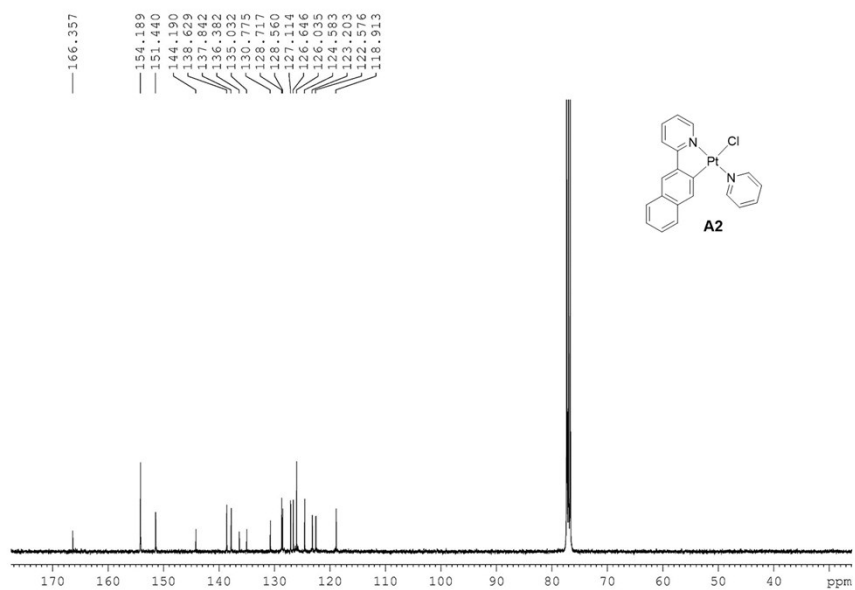
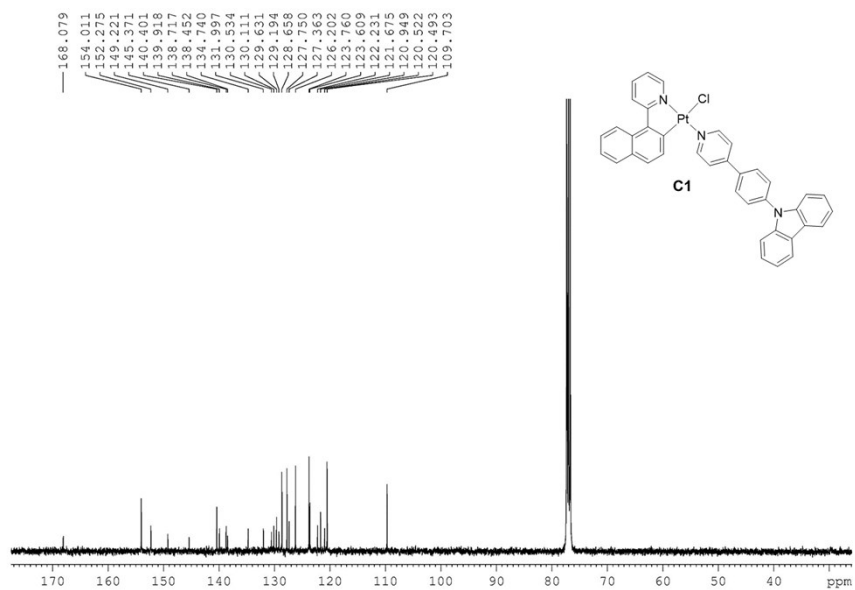


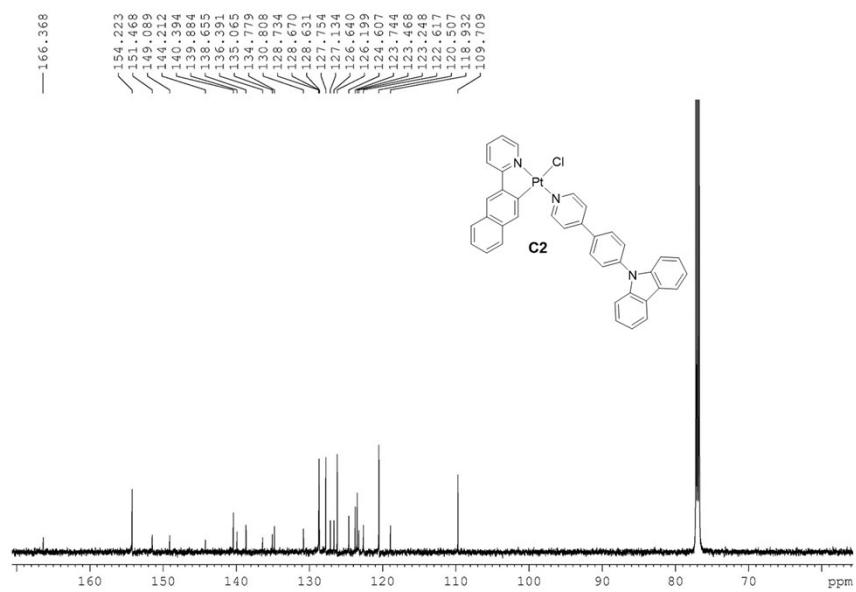
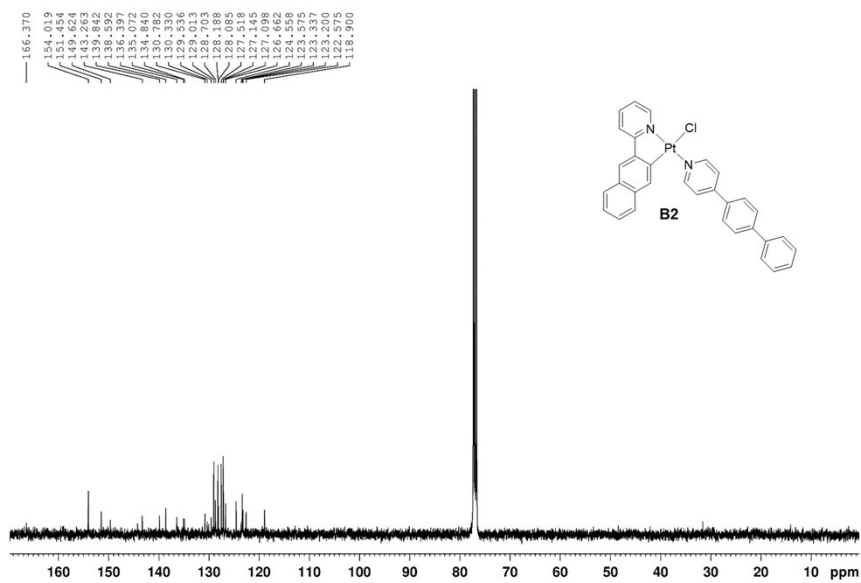
Fig. S1 ^1H NMR spectra for these $\text{Pt}^{\text{II}}(\text{C}^{\wedge}\text{N})(\text{N-donor ligand})\text{Cl}$ -type complexes.

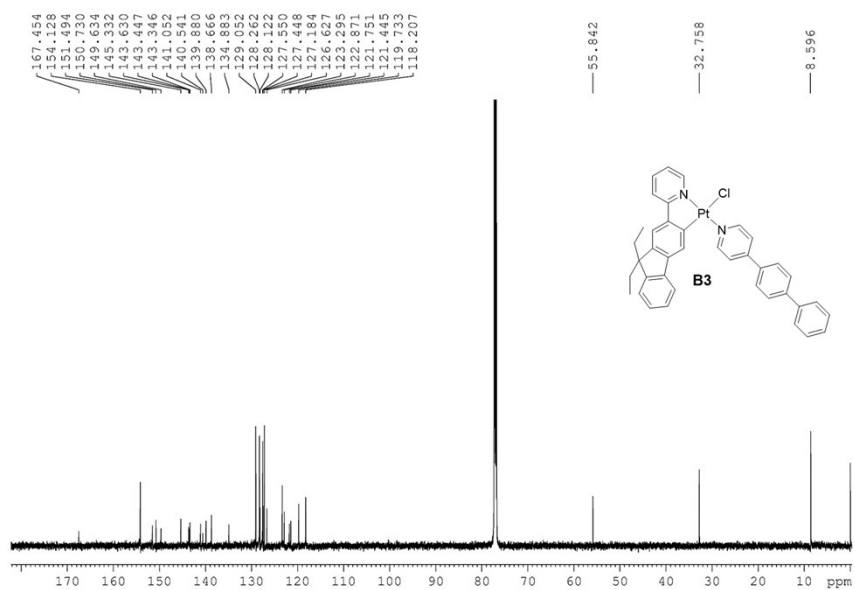
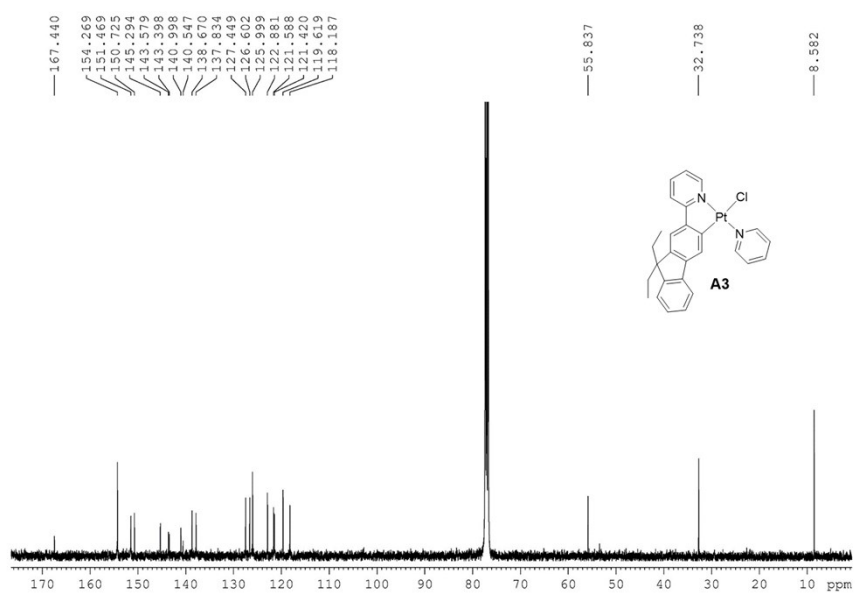
Electronic Supplementary Information



Electronic Supplementary Information







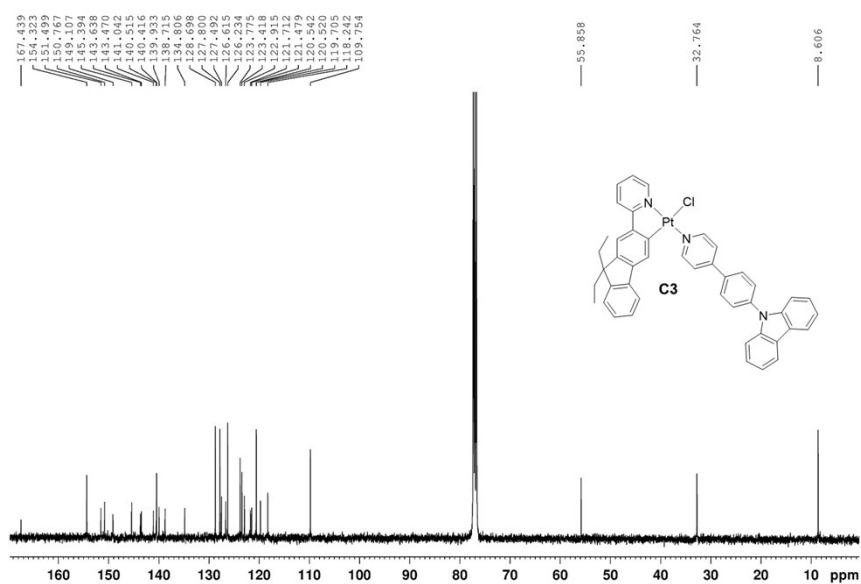


Fig. S2 ^{13}C NMR spectra for these $\text{Pt}^{\text{II}}(\text{C}^{\wedge}\text{N})(\text{N-donor ligand})\text{Cl}$ -type complexes.

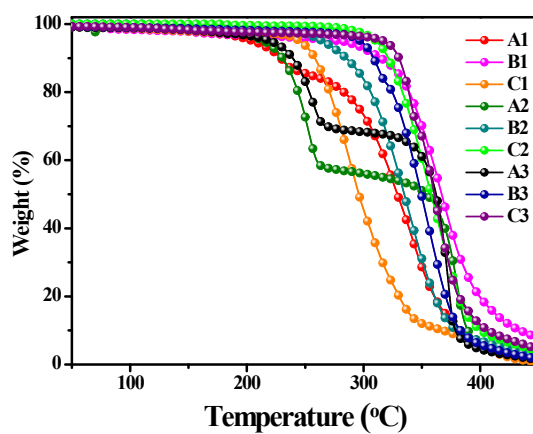


Fig. S3 The TGA curves for these $\text{Pt}^{\text{II}}(\text{C}^{\wedge}\text{N})(\text{N-donor ligand})\text{Cl}$ -type complexes.

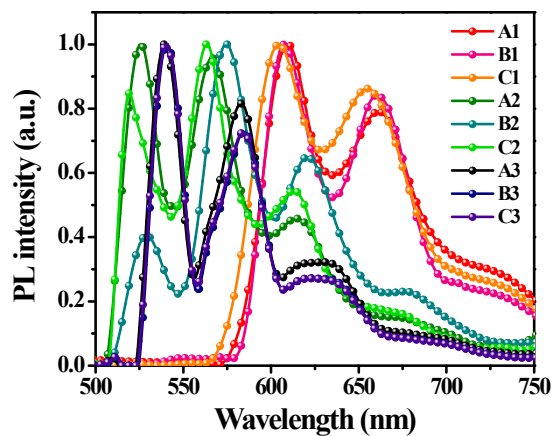
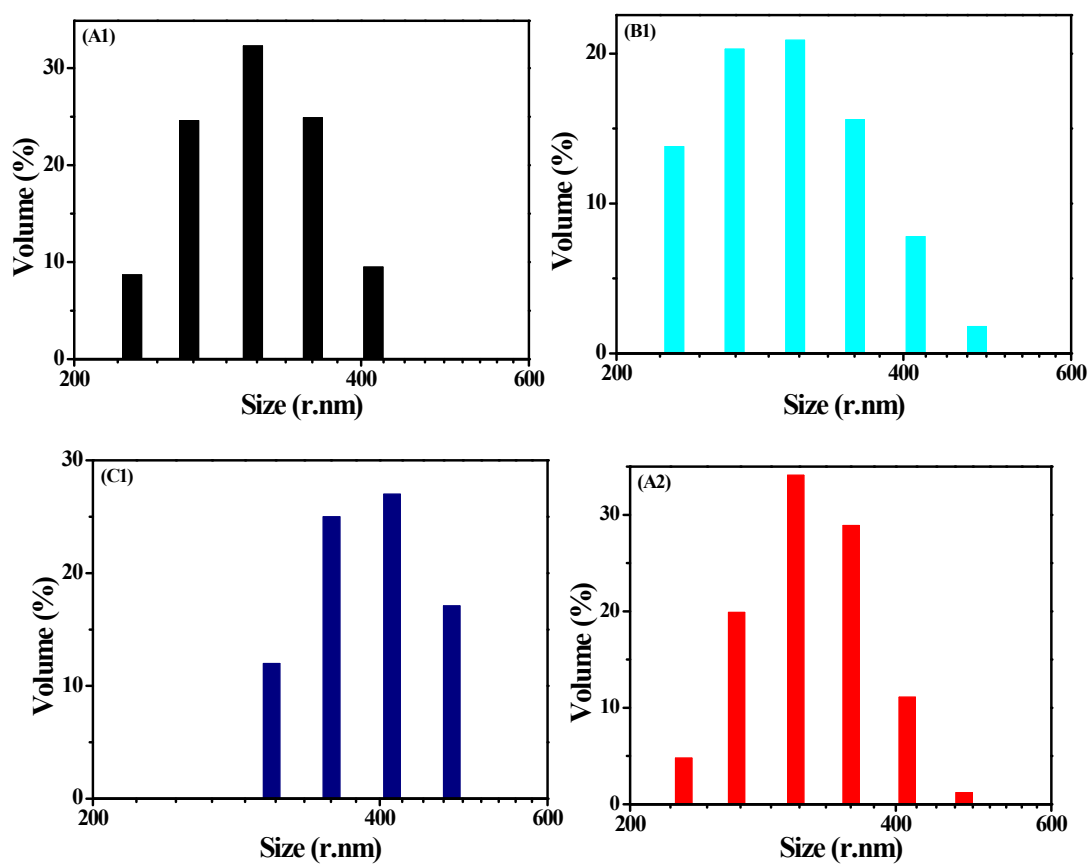


Fig. S4 Photoluminescent spectra for these Pt^{II}(C^N)(N-donor ligand)Cl-type complexes at 77K.



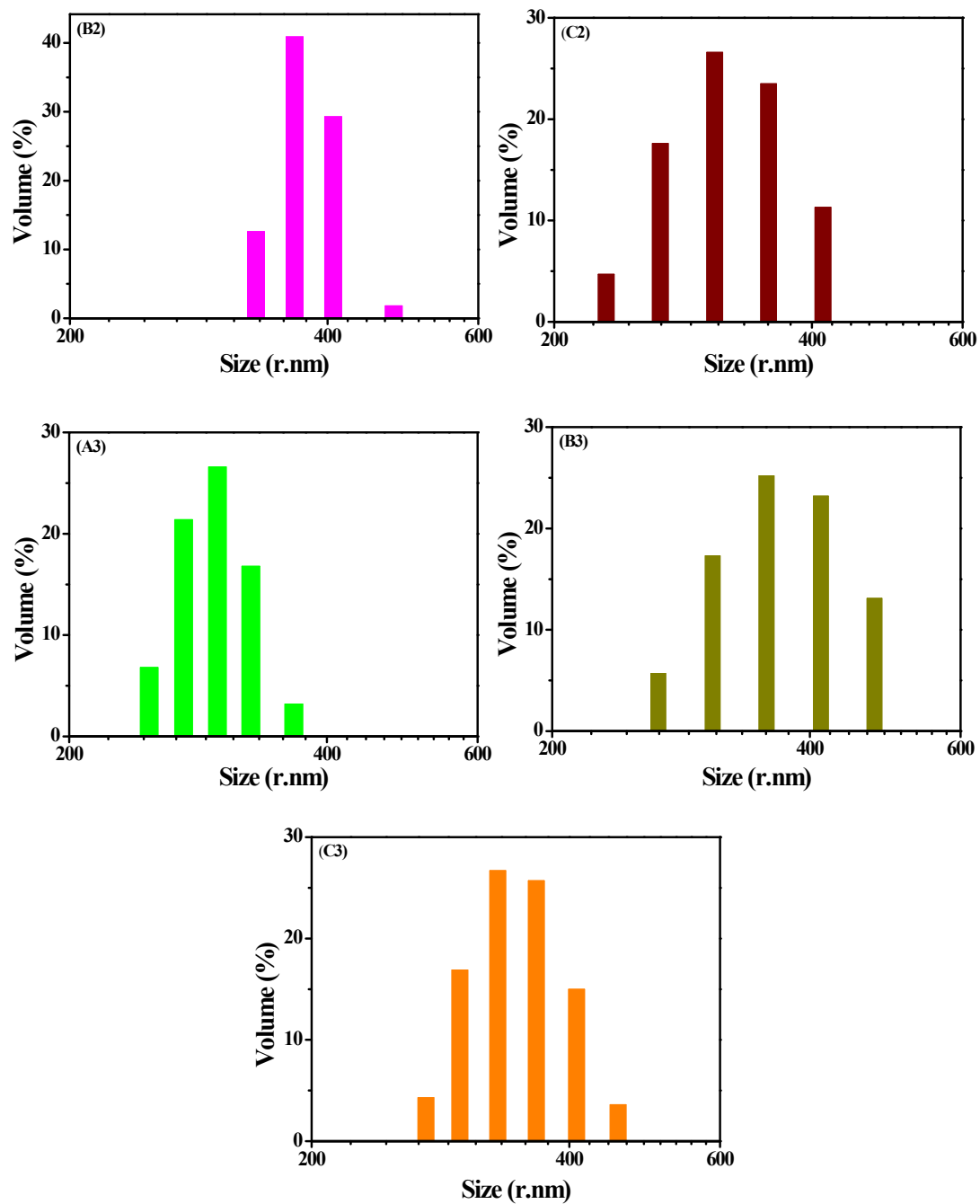


Fig. S5 Particle size distribution of these Pt^{II}(C^N)(N-donor ligand)Cl-type obtained from the THF : H₂O mixture at f_w^c .

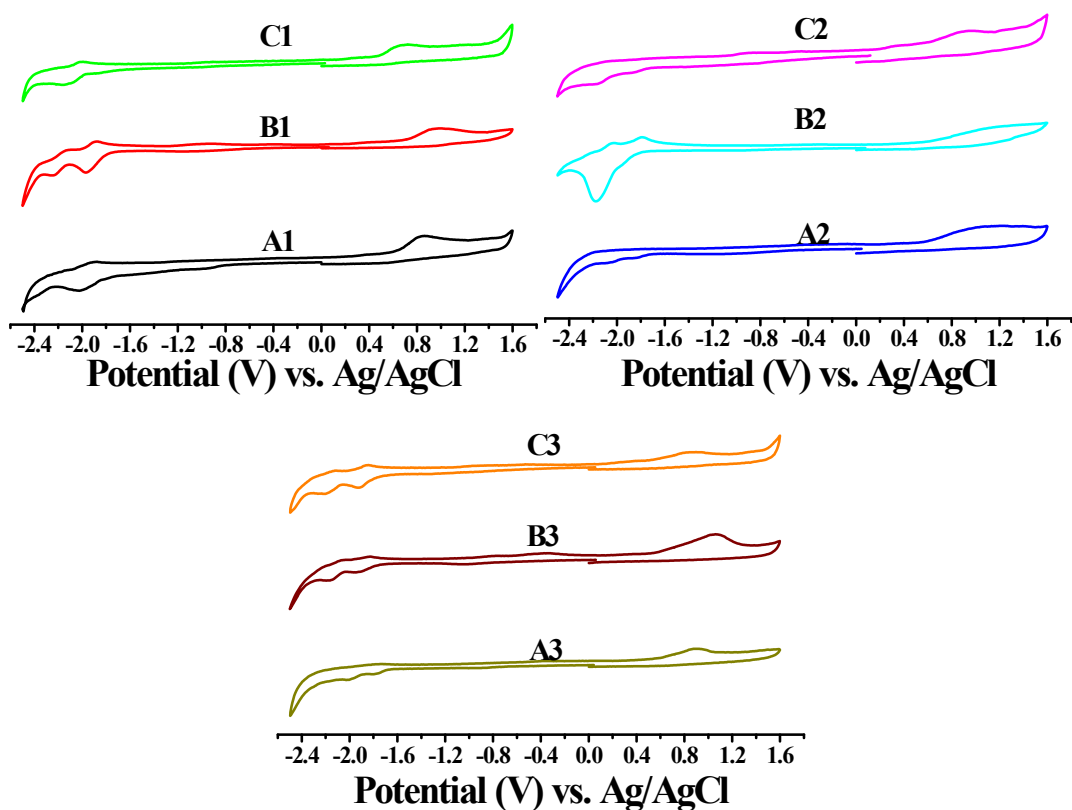
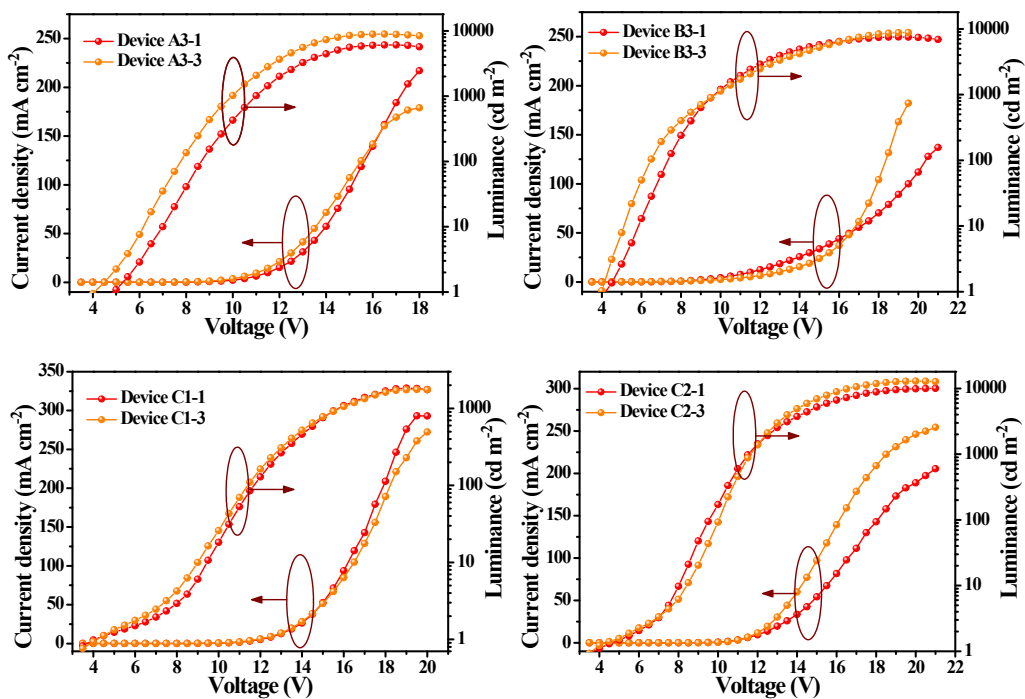


Fig. S6 CV curves for A1, B1, C1, A2, B2, C2, A3, B3 and C3



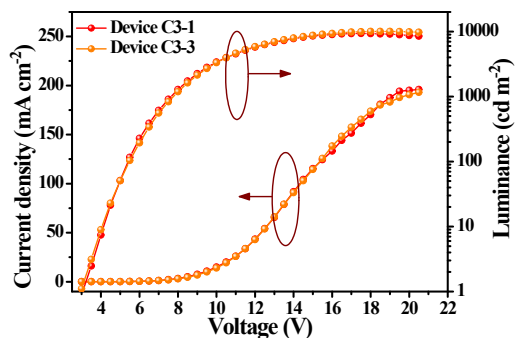
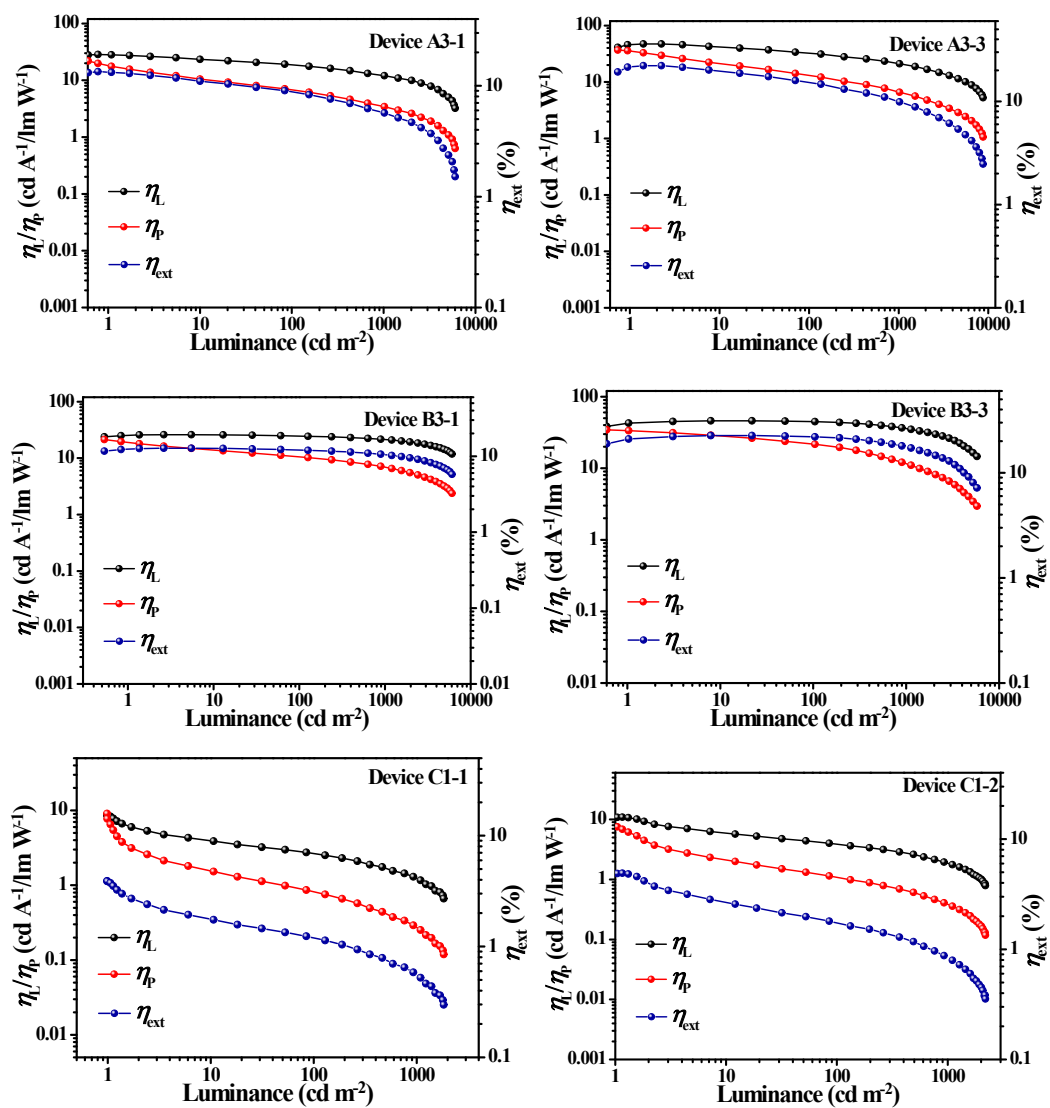


Fig. S7 Current density–voltage–luminance (J–V–L) relationships of the OLEDs.



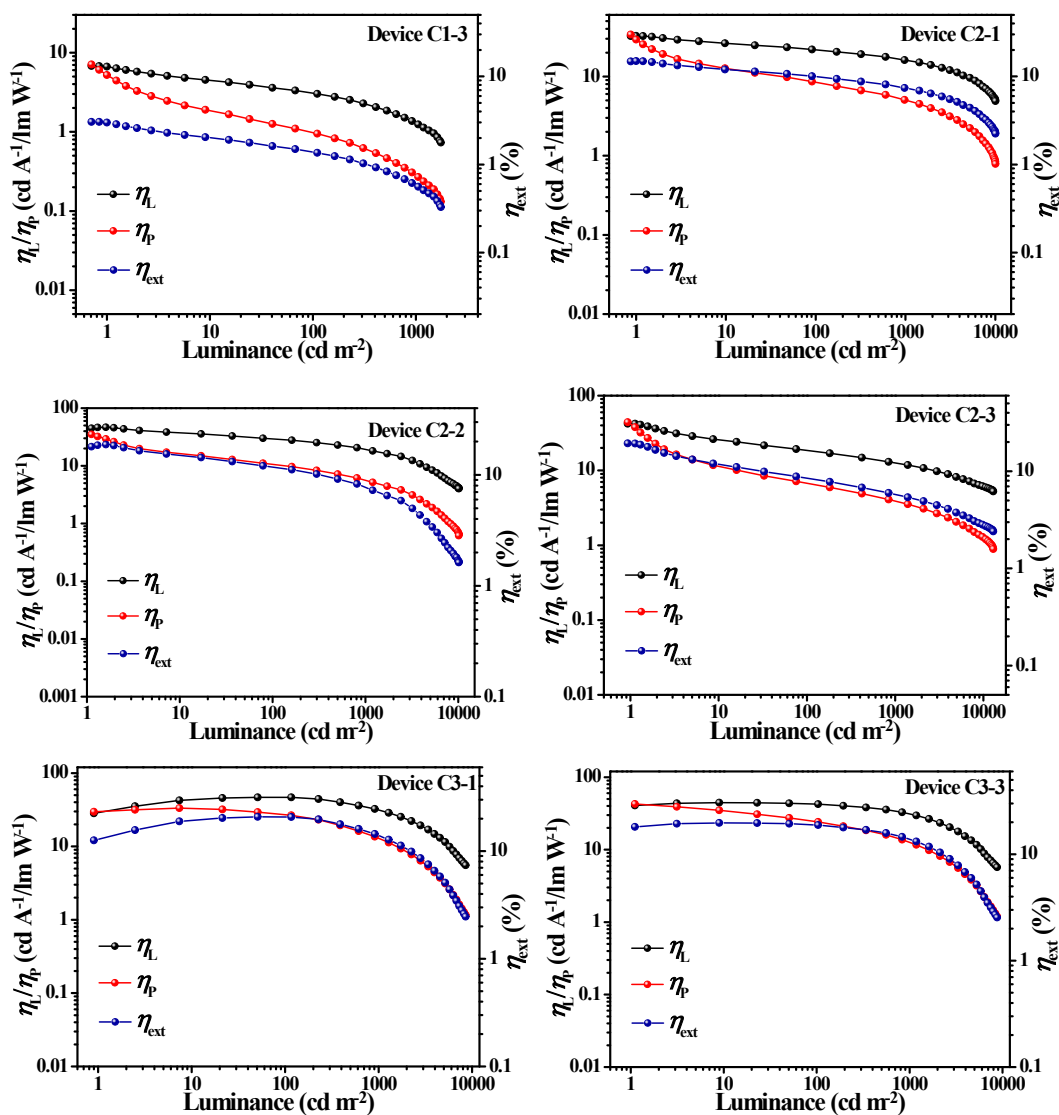


Fig. S8 EL efficiencies vs. luminance curves for the OLEDs.

References

- 1 Nunez, A. Sanchez, C. Burgos, J. Alvarez-Builla, *Tetrahedron*, 2004, **60**, 6217-6224.
- 2 X. M. Yu, G. J. Zhou, C. S. Lam, W. Y. Wong, X. L. Zhu, J. X. Sun, M. Wong, H. S. Kwok, J. *Organomet. Chem.*, 2008, **693**, 1518-1527.
- 3 O. Kobayashi, D. Uruguchi, T. Yamakawa, *Org. Lett.*, 2009, **11**, 2679-2682.
- 4 K. Leduskrasts, A. Kinens, E. Suna, *Chem. Commun.*, 2019, **55**, 12663-12666.